Available online at www.sciencedirect.com

SCIENCE DIRECT

Biochimica et Biophysica Acta 1668 (2005) 117–125

BIOCHIMICA ET BIOPHYSICA ACTA
BBA

http://www.elsevier.com/locate/bba

Formation of homogeneous unilamellar liposomes from an interdigitated matrix

Alla Polozova[a,*,1], Xingong Li[a,2], Tong Shangguan[a], Paul Meers[a,2], Daniel R. Schuette[b], Nozomi Ando[b], Sol M. Gruner[b], Walter R. Perkins[a,2]

[a]*Elan Drug Delivery, 1 Research Way, Princeton, NJ 08540, United States*
[b]*Physics Department, Cornell University, Ithaca, NY 14853, United States*

Received 3 September 2004; received in revised form 16 November 2004; accepted 17 November 2004
Available online 30 November 2004

Abstract

Phospholipid–ethanol–aqueous mixtures containing bilayer-forming lipids and 20–50 wt.% of water form viscous gels. Further hydration of these gels results in the formation of liposomes whose morphology depends upon the lipid type. Upon hydration of gels containing mixtures of the lipids 1-palmitoyl-2-oleoyl-phosphatidylcholine (POPC) and 1-palmitoyl-2-oleoyl-phosphatidylglycerol (POPG), small homogeneous and unilamellar liposomes were produced. In contrast, hydration of gels containing only POPC resulted in formation of large multilamellar liposomes. Likewise, mulitlamellar liposomes resulted when this method was applied to form highly fusogenic liposomes comprised of the novel negatively charged *N*-acyl-phosphatidylethanolamine (NAPE) mixed with di-oleoyl-phosphatidylcholine (DOPC) (7:3) [T. Shangguan, C.C. Pak, S. Ali, A.S. Janoff, P. Meers, Cation-dependent fusogenicity of an *N*-acyl phosphatidylethanolamine, Biochim. Biophys. Acta 1368 (1998) 171–183]. In all cases, the measured aqueous entrapment efficiencies were relatively high. To better understand how the molecular organization of these various gels affects liposome morphology, we examined samples by freeze-fracture transmission electron microscopy and X-ray diffraction. We found that phospholipid–ethanol–water gels are comprised of highly organized stacks of lamellae. A distinct feature of the gel samples that result in small unilamellar liposomes is the combination of acyl chain interdigitation and net electrostatic charge. We speculate that the mechanism of unilamellar liposome formation proceeds via formation of stalk contacts between neighboring layers similar to membrane hemifusion intermediates, and the high aqueous entrapment efficiencies make this liposome formation process attractive for use in drug delivery applications.
© 2004 Elsevier B.V. All rights reserved.

Keywords: Homogeneous; Liposome; Matrix

1. Introduction

Self-assembly of amphiphiles into aggregates of different morphologies has been of interest across biological, chemical and physical sciences for several decades. The ability to control self-assembly in order to produce nanoparticles of desired morphology and properties is vital for development of future nanotechnology and drug delivery. In particular, liposomes have been widely explored as drug delivery vehicles due in part to the ease with which their assembly can be manipulated to produce specifically designed carriers for a variety of different applications. Additionally, liposomes are also appealing because of their biocompatibility, ability to deliver either aqueous or hydro-

Abbreviations: POPC, palmitoyl-oleoyl-phosphatidylcholine; POPG, palmitoyl-oleoyl-phosphatidylglycerol; DOPC, di-oleoyl-phosphatidylcholine; NBD-PE, nitrobenzoxadiazol-phoshatydylethanolamine; NAPE, *N*-acyl-phosphatidylethanolamine; DPPC, di-palmitoyl-phoshatidylcholine; DSPC, di-stearoyl-phosphatidylcholine; SUV, small unilamellar vesicles

* Corresponding author. LMBB/NIAAA/NIH, 5625 Fishers Lane, Room 3N-07, Bethesda, MD 20892, United States. Tel.: +1 301 443 2716; fax: +1 301 594 0035.
E-mail address: apolozva@mail.nih.gov (A. Polozova).
[1] Present address: NIH/NIAAA, 5625 Fishers Lane, Room 3N-07, Bethesda, MD 20892, United States.
[2] Present address: Transave, Inc., 11 Deer Park Drive, Monmouth Junction, NJ 08852, United States.

0005-2736/$ - see front matter © 2004 Elsevier B.V. All rights reserved.
doi:10.1016/j.bbamem.2004.11.012

phobic therapeutics, including small molecules and large biomolecules such as DNA, and their ability to accommodate various ligands/coatings on their surface.

For the efficient entrapment of aqueous drug in liposomes, a variety of liposome formation methods have evolved; for a review, see Lasic and Papahadjopoulos [2]. In order to be encapsulated, most aqueous drugs must be included in the buffer solution during vesicle formation. For use as carriers in the systemic circulation, it has been established that liposome size should be limited to less than 200-nm diameter in order to maximize circulation lifetime [3]. Therefore, it is most desirable to form liposomes near 200 nm in diameter to avoid further processing (e.g., size reduction by extrusion [4]) which inevitably adversely affects retention of encapsulated water-soluble compounds. Although there are a few examples of 'active' or 'remote' loading processes which are highly efficient (>95%), these techniques, which involve loading of pre-formed liposomes, are limited to ionizable membrane-permeable molecules such as cationic anthracyclines [5,6].

We describe here a process by which liposomes can be produced, which exhibit both a high encapsulation efficiency and a desirable size distribution. This process involves the stepwise hydration of lipid dissolved at high concentrations in ethanol [7,8]. Recently, several other laboratories also reported the efficient encapsulation of DNA and polynulceotides (70–80%) in liposomes less than 200 nm in diameter using relatively high ratios of ethanol to lipid/water [9–11]. Lipid compositions and protocol details varied suggesting that the common link, ethanol, plays a critical role in these vesicle formation processes. While no mention of the pre-liposome characteristics was made in the above cited reports, we found that our lipid–ethanol–aqueous mixtures formed a viscous gel prior to liposome formation.

A similar viscous gel was previously observed when we added ethanol to small unilamellar vesicles (SUVs) comprised of saturated chain lipids (e.g., DPPC, DSPC) [12–14]. Evaluation of those particular intermediary gels revealed that the precursor SUVs had fused into stacked planar interdigitated-bilayer sheets which formed large liposomes upon heating the suspension to above the gel-to-liquid crystalline phase transition temperature of the lipid. We established that without the induction of interdigitation by ethanol, or by hydrostatic pressure [15], those gels would not form. While in the current study we are using unsaturated lipids which are not expected to undergo interdigitation [16], there has been evidence that monounsaturated lipids are capable of ethanol-induced acyl chain interdigitation under the appropriate conditions [17]. To gain more insight into the nature of the lipid–ethanol–aqueous gels and their influence upon the resulting liposome morphology, we detailed the conditions for gel and liposome formation and explored the molecular organization and structural transitions of phospholipid–ethanol–water mixtures by freeze-fracture electron microscopy and X-ray diffraction.

2. Materials and methods

POPC, POPG, DOPC, *N*-dodecanoyl-di-oleoyl-phosphatidylethanolamine (referred to here as NAPE) and nitrobenzoxadiazol-phoshatidylethanolamine (NBD-PE) were purchased from Avanti Polar Lipids (Alabaster, AL); cholesterol, all buffer salts and solvents were obtained from Sigma-Aldrich (St. Louis, MO). All buffer salts were Sigma Ultra grade. Deionized water and HPLC grade solvents were used in all experiments.

To prepare lipid–ethanol–buffer mixtures, dry powdered lipids were dissolved in appropriate amounts of ethanol. For samples subjected to lamellarity analysis, the fluorescent lipid NBD-PE was included at 0.2 mol% of total lipid. After the lipids were completely dissolved in ethanol, appropriate amounts of buffer were added and the mixtures vigorously vortexed.

2.1. Compositional analysis of lipid–ethanol–water gels

In samples exhibiting macroscopic phase separation, the fluid and gel portions were analyzed for lipid and ethanol as a function of temperature. Samples were placed in microcentrifuge tubes and incubated in a circulating water bath at each given temperature for 30 min. Samples were then centrifuged for 15 min at 2000 rpm in a temperature-controlled Eppendorf microcentrifuge, equilibrated at appropriate temperature, and placed in a water bath for an additional 15-min incubation. About 10-μL aliquots of fluid and gel portions of the samples were taken, placed into snap-closure microcentrifuge tubes and immediately sealed. After the weight of the aliquots was recorded, 1 ml of deionized water was placed into each tube, the contents were mixed and the tubes were kept tightly sealed. Phosphatidylcholine concentration in the samples was determined by choline assay (Wako Diagnostics, Richmond, VA). Ethanol concentration was determined using an ethanol kit assay (Sigma-Aldrich). Amount of water in each aliquot was deduced from the weight balance of all components.

2.2. Liposome analysis

Size of the liposomes was measured by dynamic light scattering using Nicomp Submicron Particle Sizer 370 (Nicomp Particle Sizing Systems, Santa Barbara, CA). Lamellarity of liposomes was measured using a NBD-PE dithionite reduction assay [18] in a microplate format. Briefly, the liposomes were placed in microplate wells at approximately 1 mM lipid concentration. Each sample was pipetted into six wells, of which three wells were treated with dithionite and three wells served as controls. Dithionite solution was pipetted into the appropriate wells of the microplate, contents were quickly mixed and the measurements were initiated immediately. Fluorescence intensity was monitored over a period of at least 30 min,

to make sure that dithionite-induced reduction of fluorescence intensity had reached a plateau in signal intensity. Upon completion of the measurement, all samples were solubilized by Triton X100 (1% final concentration in each well). The final fluorescence intensity was recorded and percentage of lipid on the outer shell of liposomes was calculated as:

$$\%L_{out} = 100^*(I_o - I)/(I_{os} - I_s),$$

where I_o and I are the intensities of control and dithionite treated samples at 30 min after addition of dithionite, and I_{os} and I_s are the intensities of detergent-solubilized control and dithionite-treated samples.

2.3. Freeze-fracture transmission electron microscopy

Ten-microliter aliquots of samples were sandwiched between copper plates, excess fluid was removed with filter paper, and the specimen was quickly frozen by plunging it into liquid propane. Freeze-fracturing and shadowing with platinum and carbon were performed in Balzers BAF 400 chamber. Replicas were viewed in JEOL JEM-1200EX transmission electron microscope at 120-kV accelerating voltage.

2.4. X-ray diffraction

Cu K_α X-rays were generated using a Rigaku RU-300 rotating anode X-ray generator equipped with a microfocus cup. The resultant X-ray beam was Ni-filtered and then focused by crossed Franks mirrors. X-ray diffraction images were obtained with a custom CCD X-ray detector similar to that described in Ref. [19]. Diffraction image spacings were calibrated with silver stearate (long spacing=48.68 Å). NAPE–DOPC–buffer samples were prepared for X-ray diffraction by transferring the mixture with a micropipette into 1.0-mm diameter glass X-ray capillaries whose narrow ends had been flame-sealed. The capillaries were spun briefly in a table-top centrifuge to settle the sample and then capped with epoxy to prevent solvent evaporation. POPC–POPG gels were heated at approximately 60 °C for 20 min to dissolve the gel state before samples were transferred into capillaries, as described above. The capillaries were held on X-ray specimen stage in a thermostated copper jacket.

3. Results

3.1. Compositional diagrams and compositional analysis

To investigate the behavior of lipid–ethanol–water mixed systems, we mapped compositional diagrams on the basis of visual inspection of samples. Solutions of lipid in ethanol at different proportions ranging from 70% to 5% lipid by weight were titrated with buffer in 10–20-μL increments. After each addition of buffer, the samples were tightly sealed, rigorously vortexed and allowed to equilibrate for 5–10 min. The macroscopic appearance of each sample was recorded. Compositional diagrams constructed for POPC

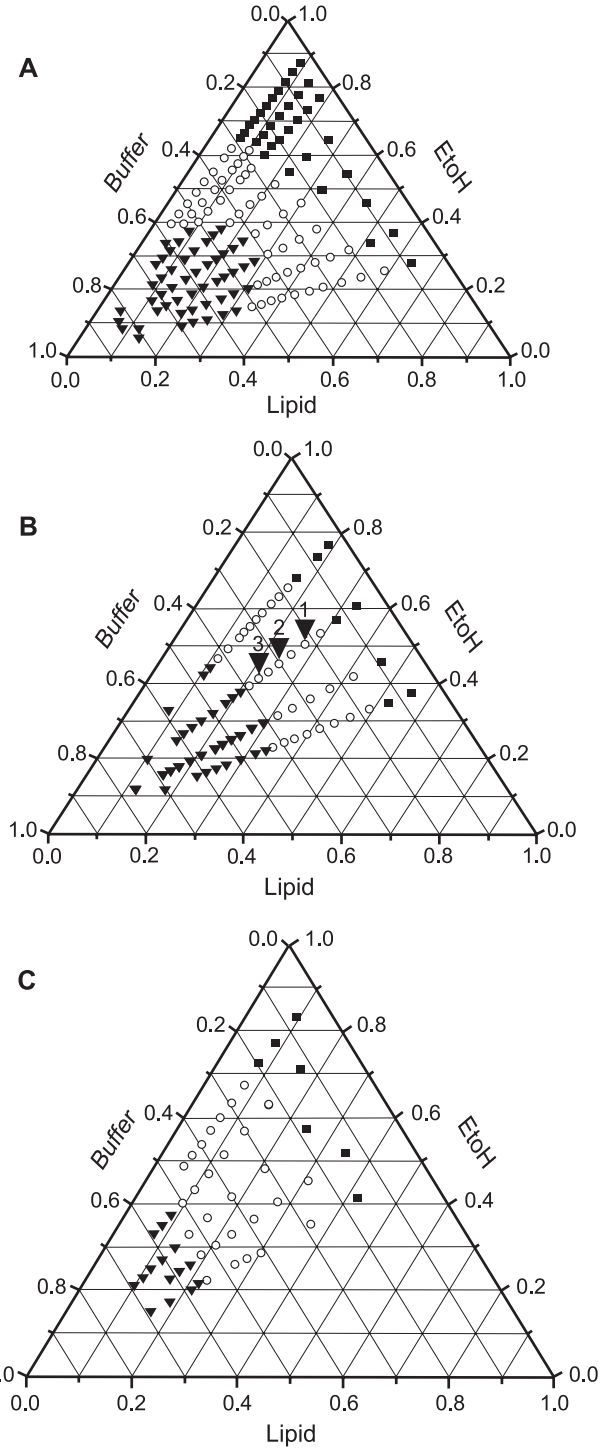

Fig. 1. Compositional diagrams depicting appearances of ethanol–aqueous buffer mixtures with (A) POPC; (B) POPC–POPG (9:1, mol/mol); (C) POPC–POPG (95:5, mol/mol). (■) Solution; (○) gel; (▼) liposomes. Buffer solution was comprised of 100 mM Tris at pH 7. Points labeled 1, 2 and 3 in (B) identify compositions used for X-ray diffraction; see text.

and POPC–POPG mixtures are presented in Fig. 1. All samples exhibited three distinctive states: (1) clear solution, (2) gel (either clear or cloudy) and (3) liposome suspension. The gel state was easily distinguished from the solution state by its high viscosity and ability of the sample to retain its shape upon inversion of vessel holding the sample. Liposome suspensions also had a very characteristic fluid milky appearance, due to production of a subpopulation of larger liposome structures. Common features to all diagrams were both the presence of a gel region in the range from approximately 25% to 50% aqueous component and the extension of the gel region to higher proportions of water at both low and high ethanol concentrations. NAPE–DOPC formed macroscopic gels upon combination with ethanol at 30–90 wt.% and aqueous buffer at 25–50 wt.%. To better understand the nature of these gel phases, we focused our investigation upon POPC–POPG and NAPE–DOPC mixtures due to their broad value for drug delivery and transfection applications [1,8].

A distinctive feature of POPC and POPC–POPG gel-containing samples was a macroscopic phase separation into fluid and gel portions, which became more pronounced at higher proportions of ethanol. In contrast to these lipid systems, NAPE–DOPC mixtures always produced homogeneous, uniform and stable gels. Macroscopic phase separation into fluid and gel parts for POPC and POPC–POPG samples began right after vortexing of the samples. Typically, a translucent gel formed and was completely settled on the bottom of the sample tube in 5–10 min. Subsequent rigorous mixings and centrifugations of the samples up to 5000 rpm did not affect fluid/gel proportions in the samples, thus suggesting that an equilibrium condition had been reached. For samples with higher ethanol proportions, the macroscopic fluid fraction increased concomitantly. The fluid portion of the samples also increased at higher temperatures until complete dissolution of the gel, which occurred above 50 °C (Fig. 2). We extracted gel portions from several samples and measured lipid and ethanol concentrations in them (see Materials and methods). We found that the ethanol/lipid ratio in gel fractions increased with temperature and with the total amount of ethanol present in samples (Table 1). At the onset of gel formation, water associated with gel was only in the range of 13–15 molecules per lipid molecule, and this proportion increased gradually with an increased total proportion of water in the samples. However, ethanol/lipid

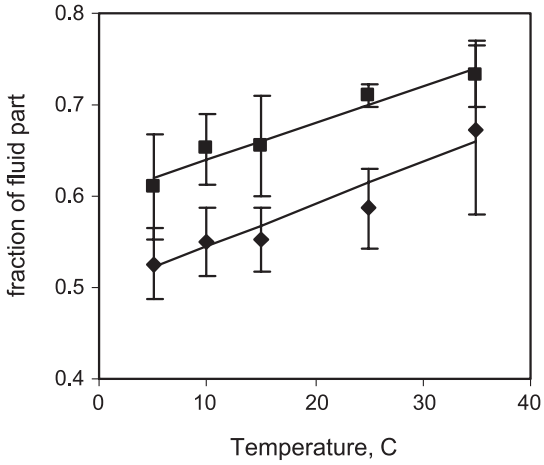

Fig. 2. Fraction of fluid part in gel-containing lipid–ethanol–buffer samples as a function of temperature. Lipid composition of samples was POPC–POPG (9:1, mol/mol); ethanol/lipid proportions were (♦) 3:2 and (■) 7:3 (w/w).

Table 1
Molar ethanol/lipid ratio in gel fractions[a] as a function of temperature and sample composition

Total ethanol/lipid (w/w)	Ethanol/lipid (mol/mol) in gel		
	5 °C	15 °C	35 °C
3:2	7±1.6	9±1.6	12±3.2
7:3	13±1.03	15±2.1	18±3.1

[a] The POPC–POPG (9:1) sample was used for the analysis. Fluid and gel parts of each sample were analyzed as described in Materials and methods.

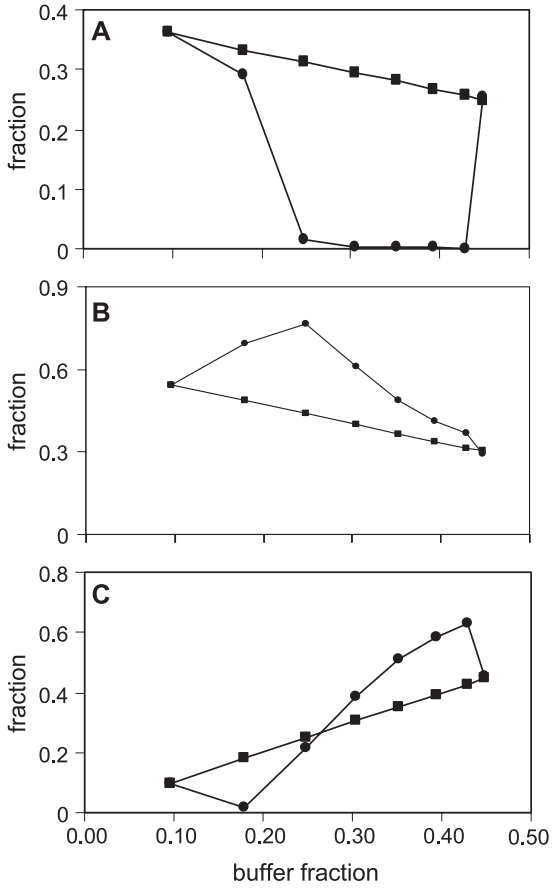

Fig. 3. Composition of fluid part (solution outside gel) for lipid–ethanol–buffer samples comprised of POPC–POPG (9:1, mol/mol). The measured (●) values for the amount of lipid (panel A), ethanol (panel B), and aqueous buffer solution (C) are compared to the expected values (■) for each where an ideal distribution throughout the total sample volume is assumed. Values are expressed as weight fractions.

ratios in gels remained nearly constant at different levels of hydration.

We next measured concentrations of lipid and ethanol in the fluid fraction at different hydration levels of the POPC–POPG (9:1) sample containing ethanol at 4:1 (w/w) proportion to the lipid. In Fig. 3 the measured proportions of lipid, ethanol and aqueous in the fluid fraction are compared to the expected concentrations, if those substances were ideally distributed throughout the sample volume. We found that essentially all of the lipid resided in the gel part of the samples, as observed in Fig. 3A. Only at the onset of gel formation could we find a significant amount of lipid (6–10%) in the fluid part. At higher levels of hydration, the lipid concentration in the fluid portion of samples quickly declined to zero and remained at this level until onset of liposome formation. Ethanol levels within the fluid phase increased initially while the overall sample concentration of ethanol declined. This indicated that ethanol predominately partitioned into the fluid portion of the samples and was excluded to some degree from the gel as it hydrated (Fig. 3B). This is reflected in the inordinate partitioning of water away from the fluid fraction and into the gel at the lower aqueous fractions seen in Fig. 3C. Above 25 wt.% of buffer solution, added buffer solution contributes preferentially to the fluid phase fraction.

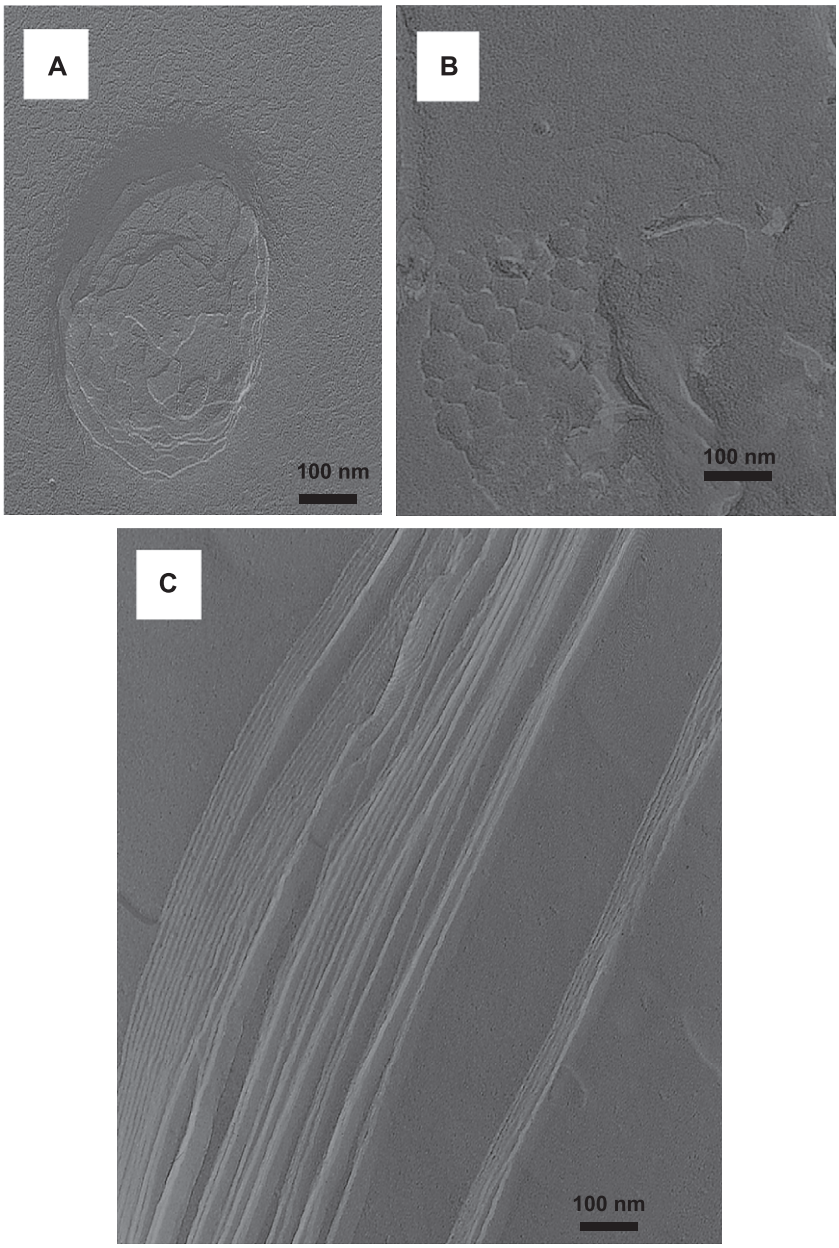

Fig. 4. Freeze-fracture transmission electron microscopy images of lipid–ethanol–buffer gel samples based on (A and B) POPC–POPG (9:1, mol/mol) and (C) NAPE–DOPC (7:3, mol/mol).

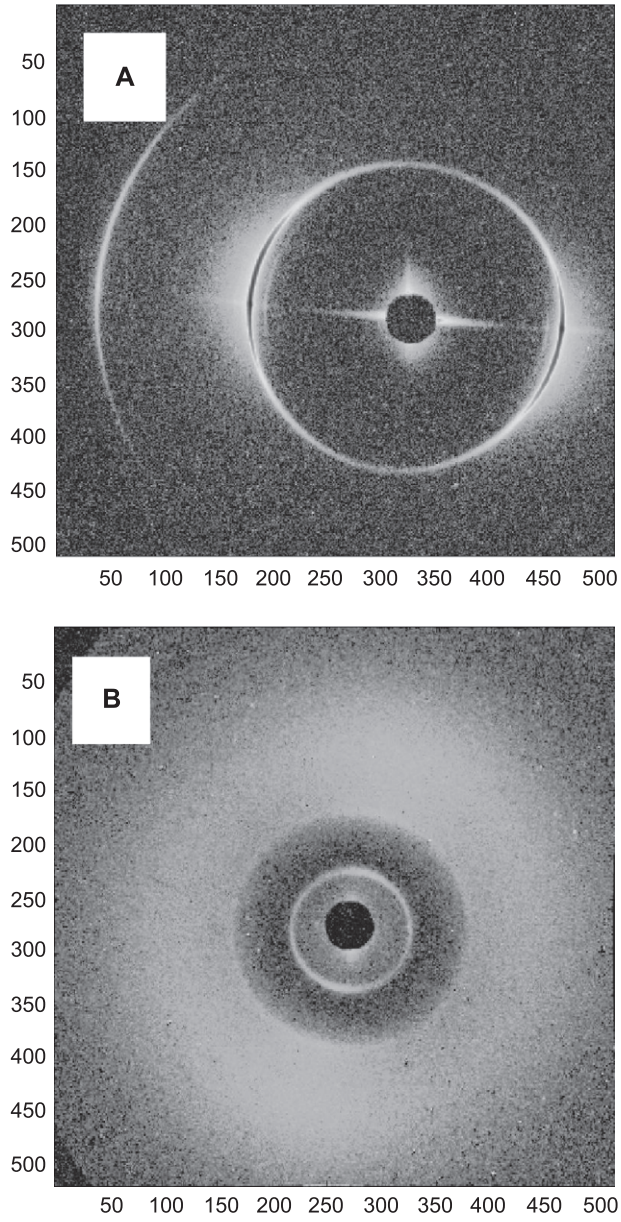

Fig. 5. X-ray diffraction patterns of lipid–ethanol–buffer gel samples at based on (A) POPC–POPG (9:1, mol/mol) sample containing 28 wt.% buffer and 43 wt.% ethanol, and (B) NAPE–DOPC (7:3, mol/mol) sample containing 40 wt.% buffer and 38 wt.% ethanol. Diffraction patterns were obtained at 30 °C.

3.2. Electron microscopy of gels

To visualize the structural organization within these gels, we examined samples by freeze-fracture transmission electron microscopy (for replica preparation details, see Materials and methods). The predominant structures observed in lipid–ethanol–water gels appeared to be extended flat multilayers (Fig. 4). For a gel made with POPC–POPG (9:1, mol/mol), surfaces of what appeared to be multilayers exhibited rough appearance (Fig. 4A), while multilayers observed in the NAPE–DOPC (7:3, mol/mol) sample were very smooth (Fig. 4C). Layers in the POPC–POPG-containing gel seemed very thin with curved irregular edges. By comparison, the bilayer packing observed for the NAPE–DOPE sample appeared to be more regularly aligned with straight edges (Fig. 4A and C). For the POPC–POPG-containing gel samples, we also observed abundant comb-like structures or clusters of semi-spherical particles (Fig. 4B). Individual units in such clusters were about 50–200 nm in cross-section length; these units may be liposome precursors; see Discussion.

3.3. X-ray diffraction of gel

POPC–POPG- and NAPE–DOPC-containing gel samples were analyzed by X-ray diffraction. Each lipid mixture was examined at three different levels of gel hydration at a 2:3 lipid/ethanol ratio (points 1, 2 and 3 in Fig. 1B). All POPC–POPG gel samples exhibited very sharp diffraction patterns characteristic of regularly spaced multilamellar structure in which lamellae were predominantly aligned in one direction, presumably due to shear alignment when the sample was transferred to the X-ray capillaries (Fig. 5A). Diffraction patterns of NAPE–DOPC-based samples were also of typical lamellar character, but in contrast to the patterns for POPC–POPG samples, the lines consisted of weaker, sharp maxima superimposed on broad diffuse scatter (Fig. 5B). After heat cycling, both the sharp and diffuse features were circularly symmetric, indicating no tendency toward macroscopic alignment.

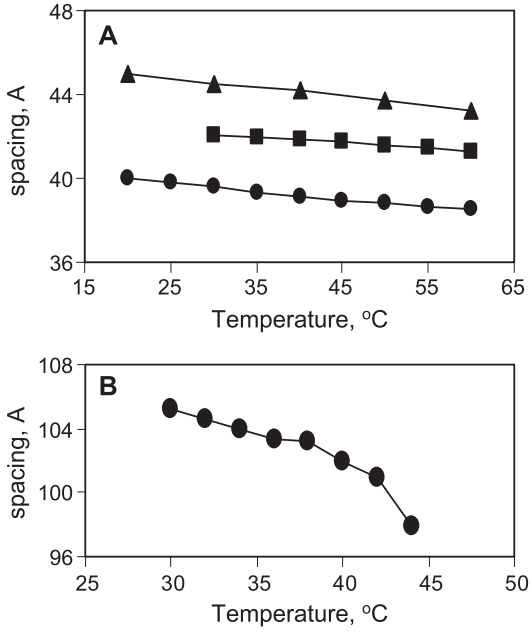

Fig. 6. Repeat spacings observed for lipid–ethanol–buffer gels as a function of temperature. Samples contained (A) POPC–POPG (9:1, mol/mol) and (●) 20, (■) 28, (▼) 37 wt.% of 100 mM Tris buffer (pH=7); (B) NAPE–DOPC (7:3, mol/mol) lipid mixture and 40 wt.% of 10 mM Tris buffer containing 1 mM NaCl (pH=7).

As shown in Fig. 6, lamellar repeat spacings (i.e., the lamellar basis vector lengths) were dependent on temperature and amount of water in the samples. Spacings for POPC–POPG-containing samples increased as water content was increased: from 40 to 45 Å at 20 °C on going from 20% to 35% water. For all levels of hydration, the spacings decreased modestly (1–2 Å at 60 °C) with increasing temperature. A similar trend was observed for NAPE–DOPC sample, but repeat spacing values were more than twice as large, in the range of 104–98 Å, and the decrease in repeat spacing was more exaggerated at higher temperature (Fig. 6B).

3.4. Size and lamellarity of the liposomes produced by gel hydration

Size and morphology of the liposomes resulting from hydration of the gels were dependent on the lipid type and lipid composition. Hydration of gels containing only POPC or the NAPE–DOPC mixture resulted in the formation of large multilamellar liposomes with less than 1.5 L/mol captured aqueous volumes. Surprisingly, liposomes formed from gels containing POPC–POPG mixtures were predominately unilamellar and 100–200 nm in size (see Table 2).

Morphological characteristics of the liposomes formed from POPC–POPG-containing gels were independent of hydration method. We compared liposomes formed from a 2:3 lipid/ethanol system either by slow dropwise titration of buffer or by rapid mixing of the gel with a sufficiently large amount of buffer to cross the gel–liposome boundary (see Fig. 1). We found that in both cases the liposomes were in the 100–200-nm size range and had similar 5–7 L/mol captured volumes. Encapsulation efficiency of water-soluble compounds, evaluated as the amount of material remaining inside the liposomes after hydration of gel with empty buffer, was dependent on initial proportion of water in the gel. For a sample corresponding to point 1 on the compositional diagram of Fig. 1, the entrapment efficiency was 10%, while for a sample corresponding to point 2, the value was 67%.

Table 2
Properties of liposomes formed by hydration of ethanol–lipid–water gels

Mixture type	Lipid/ ethanol	Size, nm		Percentage of lipid on the outer shell of the liposomes	Captured volumes, L/mol
		Average	Populations		
POPC–POPG (9:1)	3:2	350	180 (90%), 1000 (10%)	46±4	6.6
	1:1	550	200 (85%), 1000 (15%)	46±5	7.1
	1:4	860			7.0
POPC–POPG (95:5)	2:3	410	220 (70%), 600 (30%)	27±1.4	3.2
	3:7	690	195 (76%), 1000 (24%)	29±0.8	3.8
	1:9	420	100 (87%), 800 (13%)	29±1.3	1.5

4. Discussion

According to electron micrographs and X-ray diffraction data, lipid–ethanol–water gels are highly organized stacks of lamellae. Relatively short repeat distances were detected for gels containing POPC–POPG mixtures (<46Å). The thickness of only the hydrophobic core of a POPC bilayer has been reported to be around 40 Å [20], while typical spacings for fully hydrated bilayers are over 60 Å [21]. Such low values as those observed here, however, have been reported for bilayer membranes existing in an interdigitated state where there is a significant degree of acyl chain overlap [16]. While examples of acyl chain interdigitation had been confined to only saturated chain lipids, McIntosh et al. [17] recently reported that ethanol can induce acyl chain interdigitation for phosphatidylcholine bilayers comprised of di-C20 lipids possessing a single *cis* double bond along the *sn*-2 acyl chain. Therefore, it is not unreasonable to assume that ethanol participates in the structural organization of POPC–POPG bilayers into an interdigitated state. For the induction of interdigitation, ethanol partitions into the bilayer at the interfacial region and shields what would otherwise be the exposed hydrophobic acyl chains of the lipid from the opposite monolayer. For the POPC–POPG mixtures in this study, conditions of limited hydration and high ethanol concentration could cause the acyl chains to adopt an all-*trans* conformation, typical of gel bilayer state. This would then allow the organized packing associated with interdigitation.

POPC–POPG samples exhibited macroscopic phase separation, probably due to rapid self-assembly of large interdigitated layers. These multilayers obviously formed the body of the gel, and our data indicate that below a certain minimum threshold of water (~25% under the conditions of Fig. 3), any added water was preferentially absorbed by the gel fraction. As evidenced by the diffraction data of Fig. 6, lamellar repeat spacings were noted to increase with increasing levels of hydration. The simplest explanation is that the interbilayer distances were increasing due to swelling between the layers, but we cannot rule out changes in lipid packing such as lipid orientation (tilt) or the degree of chain overlap to explain the data.

At sufficiently high levels of hydration there may be insufficient ethanol per lipid to sustain interdigitation (i.e., an energetically unfavorable situation arises as acyl chain ends gain more exposure to water). Consequently, the interdigitated layer converts into non-interdigitated bilayer. It is likely that it is at this point that liposome formation occurs since we know from our previous studies with interdigitated saturated bilayers that liposome formation

does not occur until the bilayer adopts the liquid-crystalline (L_α) phase [3,14]. Transition of the originally rigid interdigitated layer into a non-interdigitated bilayer (L_α) and the initiation of vesicular structures may occur via formation of stalk contacts between the neighboring layers (Fig. 7), through intermediates similar to those recently described for membrane fusion [22]. It was shown that short-chain alcohols such as methanol and ethanol promote formation of stalk contacts and membrane hemifusion [23]. Formation of contacts between adjourning layers might be preferential due to lower curvature strain, as compared to formation of vesicles from bilayer patches formed inside one interdigitated layer. The honeycomb-like structures observed for gel replicas by electron microscopy would be consistent with the presence of circular interlayer contacts. These structures may seed formation of unilamellar liposomes at sufficiently high hydration levels. Formation of predominately small (100–200 nm) unilamellar liposomes was observed for all samples based on POPC–POPG mixtures.

Vesicle morphology (size, the average number of lamellae per liposome, and captured volume) appeared to be affected by the amount of POPG present in the mixture, as seen in Table 2. For systems with only 5 mol% POPG, captured volume was lower and the number of layers per liposome was higher. For POPC alone (no POPG), the resulting liposomes were highly multilayered (data not shown). These data suggest that the presence of the charged lipid may play a role in the vesiculation process. However, it is not clear to us at this time how the bilayer charge may influence the liposome formation process.

While the NAPE–DOPC (7:3) lipid system is also highly charged (NAPE is negatively charged), its gel microstructure is clearly very different from that of the POPC–POPG system (Fig. 4). Likewise, the resulting liposomes are highly multilayered with large interbilayer distances [8]. Although X-ray data indicate the presence of lamellae, the large repeat spacings and very diffuse diffraction lines point to a typical fluid bilayer packing of lipid molecules. The NAPE lipid is very unusual in that it possesses a C12 hydrocarbon chain attached to the headgroup and both the NAPE and DOPC lipids comprising this mixture contain di-oleoyl (18:1) chains. With two *cis* double bonds and the unusual headgroup, this system may be incapable of adopting an interdigitated state, at least under the conditions set forth here. Apparently, in the absence of interdigitation, the liposomes form in the usual way, where patches of multi-

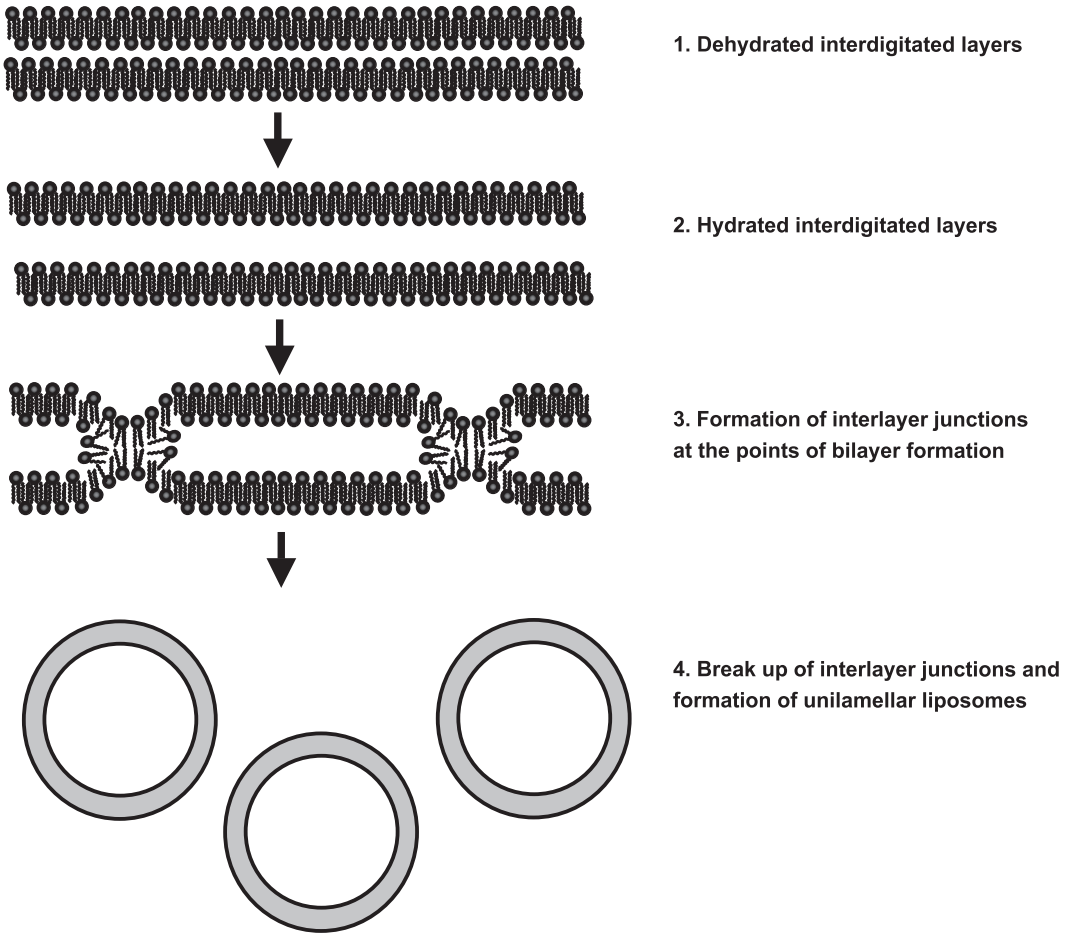

Fig. 7. Suggested mechanism of transition of interdigitated layer into unilamellar liposomes through formation of interlayer stalk contacts.

layers break down by shear forces at higher levels of hydration.

Acknowledgements

This work was supported by Elan Drug Delivery. The X-ray diffraction facility at Cornell is supported by DOE grant DE-FG02-97ER62443.

References

[1] T. Shangguan, C.C. Pak, S. Ali, A.S. Janoff, P. Meers, Cation-dependent fusogenicity of an *N*-acyl phosphatidylethanolamine, Biochim. Biophys. Acta 1368 (1998) 171–183.
[2] D.D Lasic, D. Papahadjopoulos, Liposomes and biopolymers in drug and gene delivery, Curr. Opin. Solid State Mater. Sci. 1 (3) (1996) 392–400.
[3] P.L. Ahl, S.K. Bhatia, P. Meers, P. Roberts, R. Stevens, R. Dause, W.R. Perkins, A.S. Janoff, Enhancement of the in vivo circulation lifetime of L-α-distearoylphosphatidyl-choline liposomes: importance of liposomal aggregation versus complement opsonization, Biochim. Biophys. Acta 1329 (1997) 370–382.
[4] L.D. Mayer, M.J. Hope, P.R. Cullis, Vesicles of variable size produced by a rapid extrusion procedure, Biochim. Biophys. Acta 858 (1986) 161–168.
[5] T.D. Madden, P.R. Harrigan, L.C.L. Tari, M.B. Bally, L.D. Mayer, T.E. Redelmeier, H.C. Loughrey, C.P.S. Tilcock, L.W. Reinish, P.R. Cullis, The accumulation of drugs within the large unilamellar vesicles exhibiting a proton gradient: a survey, Chem. Phys. Lipids 53 (1990) 37–46.
[6] N.L. Dos Santos, D. Mayer, S.A. Abraham, R.C. Gallagher, K.A.K. Cox, P.G. Tardi, M.B. Bally, Improved retention of idarubicin after intravenous injection obtained for cholesterol-free liposomes, Biochim. Biophys. Acta 1561 (2002) 188–201.
[7] A. Polozova, X. Li, T. Shangguan, P. Meers, D.R. Schuette, N. Ando, S.M. Gruner, W.R. Perkins, Structural transitions in lipoid–ethanol–water mixtures, Biophys. J. (2002) (2470-Plat, 505a).
[8] T. Shangguan, X. Li, A. Polozova, W.R. Perkins, P. Meers, Efficient plasmid DNA encapsulation into medium sized *N*-acyl phosphatidylethanolamine-containing liposomes for gene transfer, Molecular Therapy, J. Am. Soc. Gene Ther. 5 (5) (2002) S74.
[9] A.L. Bailey, S.M. Sullivan, Efficient encapsulation of DNA plasmids in small neutral liposomes induced by ethanol and calcium, Biochim. Biophys. Acta 1468 (2000) 239–252.
[10] S.C. Semple, S.K. Klimuk, T.O. Harasym, N. Dos Santos, S.M. Ansell, K.F. Wong, N. Maurer, H. Stark, P.R. Cullis, M.J. Hope, P. Scherrer, Efficient encapsulation of antisense oligonucleotides in lipid vesicles using ionizable aminolipids: formation of novel small multilamellar vesicle structures, Biochim. Biophys. Acta 1510 (2001) 152–166.
[11] N. Maurer, K.F. Wong, H. Stark, L. Louie, D. McIntosh, T. Wong, P. Scherrer, S.C. Semple, P.R. Cullis, Spontaneous entrapment of polynucleotides upon electrostatic interaction with ethanol-destabilized cationic liposomes, Biophys. J. 80 (5) (2001) 2310–2326.
[12] L.T. Boni, S.R. Minchey, W.R. Perkins, P.L. Ahl, J.L. Slater, M.W. Tate, S.M. Gruner, A.S. Janoff, Curvature dependent induction of the interdigitated gel phase in DPPC vesicles, Biochim. Biophys. Acta 1146 (1993) 247–257.
[13] P.L. Ahl, L. Chen, W.R. Perkins, S.R. Minchey, L.T. Boni, T.F. Taraschi, A.S. Janoff, Interdigitation-fusion: a new method for producing lipid vesicles of high internal volume, Biochim. Biophys. Acta 1195 (1994) 237–244.
[14] P.L. Ahl, W.R. Perkins, Interdigitation-fusion liposomes, Methods Enzymol. 367 (2003) 80.
[15] W.R. Perkins, R.B. Dause, X. Li, T.S. Davis, P.L. Ahl, S.R. Minchey, T.F. Taraschi, S. Erramilli, S.M. Gruner, A.S. Janoff, Pressure induced fusion (PIF) liposomes: a solventless sterilizing method for producing large phosholipid vesicles, J. Liposome Res. 5 (3) (1995) 605–626.
[16] J.L. Slater, C.H. Huang, Interdigitated Bilayer-Membranes, Prog. Lipid Res. 27 (4) (1988) 325–359.
[17] T.J. McIntosh, H. Lin, S. Li, C.-H. Huang, The effect of ethanol on the phase transition temperature and the phase structure of monounsaturated phosphatidylcholines, Biochim. Biophys. Acta 1510 (2001) 219–230.
[18] J.C. McIntyre, R.G. Sleight, Fluorescence assay for phospholipid membrane asymmetry, Biochemistry 30 (1991) 11819–11827.
[19] M.W. Tate, E.F. Eikenberry, S.L. Barna, M.E Wall, J.L. Lowrance, S.M. Gruner, A large-format, high-resolution area X-ray detector based on a fiber-optically bonded charge coupled device (CCD), J. Appl. Crystallogr. 28 (1995) 196–205.
[20] H. Binder, K. Gawrisch, Effect of unsaturated lipid chains on dimensions, molecular order and hydration of membranes, J. Phys. Chem. 105 (2001) 12378–12390.
[21] H. Schmieldel, P. Jorchel, M. Kiselev, G. Klose, Determination of structural parameters at high water excess from neutron scattering curves using a novel method of evaluation, J. Phys. Chem. 105 (2001) 111–117.
[22] L. Yang, H.W. Huang, Observation of a membrane fusion intermediate structure, Science 297 (2002) 1877–1879.
[23] A. Chanturia, E. Leikina, J. Zimmerberg, L.V. Chernomordik, Short-chain alcohols promote an early stage of membrane hemifusion, Biophys. J. 77 (1999) 2035–2045.